Journal of Solid State Chemistry ∎ (∎∎∎∎) ∎∎∎–∎∎∎

Contents lists available at ScienceDirect

Journal of Solid State Chemistry

journal homepage: www.elsevier.com/locate/jssc

Hydrothermal crystal growth, piezoelectricity, and triboluminescence of $KNaNbOF_5$

Kelvin B. Chang [a], Bryce W. Edwards [b], Laszlo Frazer [c,1], Erik J. Lenferink [c], Teodor K. Stanev [c], Nathaniel P. Stern [c], Juan C. Nino [b], Kenneth R. Poeppelmeier [a,*]

[a] Department of Chemistry, Northwestern University, Evanston, IL 60208, USA
[b] Department of Materials Science and Engineering, University of Florida, Gainesville, FL 32611, USA
[c] Department of Physics and Astronomy, Northwestern University, Evanston, IL 60208, USA

ARTICLE INFO

Article history:
Received 12 May 2015
Received in revised form
7 July 2015
Accepted 9 July 2015

Keywords:
Crystal growth
Oxide-fluoride
Piezoelectricity
Triboluminescence

ABSTRACT

Single crystals of the noncentrosymmetric $KNaNbOF_5$ polymorph were grown for piezoelectric and triboluminescent measurements. Piezoelectric measurements yielded a d_{33} value of ± 6.3 pCN^{-1} and an effective electromechanical coupling coefficient of up to 0.1565 in the frequency range 1960–2080 kHz. Crystals of $KNaNbOF_5$ were found to exhibit a strong triboluminscence effect visible to the naked eye as blue sparks when crystals are crushed. This triboluminescence effect is uncommon in that it is likely independent from both the piezoelectric effect and atmospheric electrical discharge. Instead, triboluminescence may originate from crystal defects or be related to an electroluminescence effect.

1. Introduction

Triboluminescence (TL) is the release of light upon fracturing chemical bonds. Triboluminescent materials have been applied as a damage or fracture indicator in composite materials [1–3]. Triboluminescence can have multiple different origins, the most common of which are crystal fluorescence, crystal phosphorescence, and gas discharge [4]. Mechanisms for TL are not mutually exclusive, and multiple processes can occur within a single material. These mechanisms are typically thought to be linked to polarization and the creation of charged surfaces as materials are fractured, which explains why TL is often found in piezoelectric materials. Perhaps the most common example of TL are sugars such as wintergreen flavored hard candies [5,6]. When these sugars are crushed, the nitrogen gas discharge spectrum is observed [6]. The UV emission from N_2 discharge is a source of photoluminescence excitation, which creates a broad emission in the visible region. This phenomenon can be observed with the naked eye in a dark room with pupils fully dilated. It is interesting to note, however, that triboluminescence can also be observed in centrosymmetric (CS) materials such as doped fluorites [7]. TL is therefore a phenomenon with several possible origins that are not completely understood, where any one explanation cannot be applied to all triboluminescing materials.

Potassium sodium niobate (KNN) based materials are a promising candidate to replace lead based ceramics such as lead zirconate titanate (PZT) [8–10]. While the electromechanical responses of KNN based materials do not yet meet those of PZT, properties have been enhanced through doping, sintering processes, and domain engineering [7]. Strong TL in the noncentrosymmetric (NCS) polymorph of $KNaNbOF_5$, visible with the naked eye under normal lighting conditions, was observed as blue sparks when this phase was first grown. Owing to the relationship between TL and piezoelectricity, and the fact that this compound adopts a NCS structure that permits piezoelectric behavior, $KNaNbOF_5$ is examined as a potential new piezoelectric material.

Large crystals are needed to measure piezoelectricity and study triboluminescent properties. $KNaNbOF_5$ undergoes a phase transition at 350 °C to an unknown structure, [11] which precludes crystal growth from a stoichiometric melt or a flux. Crystals of $KNaNbOF_5$ can be obtained, however, from solutions under mild hydrothermal conditions. Our new synthetic procedure [11] has enabled growth of large single crystals.

Hydrothermal crystal growth entails dissolving bulk powder followed by slow precipitation to form a large single crystal. Material can be precipitated onto a seed crystal through chemical transport achieved with application of a temperature gradient

---

[*] Corresponding author.
E-mail address: krp@northwestern.edu (K.R. Poeppelmeier).
[1] Present address: Department of Chemistry, Temple University, Philadelphia, PA 19122, USA.

http://dx.doi.org/10.1016/j.jssc.2015.07.011
0022-4596/© 2015 Elsevier Inc. All rights reserved.

Please cite this article as: K.B. Chang, et al., J. Solid State Chem. (2015), http://dx.doi.org/10.1016/j.jssc.2015.07.011

[12,13]. Alternatively, the reaction can be cooled slowly for spontaneous nucleation followed by crystal growth. In either case, temperature, concentration, and pH are critical factors. Crystal growth of the NCS polymorph of $KNaNbOF_5$ faces an additional challenge since both polymorphs of $KNaNbOF_5$ can be grown hydrothermally, sometimes from the same solution [11,14–17]. Because hydrothermal crystal growth can take multiple days to weeks to obtain large single crystals, crystal growth conditions that ensure the correct polymorph crystallizes must also be targeted. This work describes the hydrothermal single crystal growth of $KNaNbOF_5$. Large single crystals allowed measurements of triboluminescent and piezoelectric properties.

2. Material and methods

2.1. Crystal growth

Caution: Hydrofluoric acid is toxic and corrosive, and must be handled with extreme caution and the appropriate protective gear! If contact with the liquid or vapor occurs, proper treatment procedures should immediately be followed [18–20].

The compounds Nb_2O_5 (99.9% Aldrich), NaF (99%, Aldrich), KNO_3 (99.9%, Mallinckrodt), $NaNO_3$ (99.0%, Alfa Aesar) and aqueous hydrofluoric acid (HF) (48% HF by weight, Aldrich) were used as received. Deionized water was used in the syntheses. All reactants were sealed in Teflon [fluoro(ethylenepropylene), FEP] “pouches” as previously described [21]. Pinholes on the top of these pouches were made using a needle. Four to six pouches were placed in a 125 mL Teflon-lined Parr pressure vessel filled with 42 mL of deionized H_2O as backfill. Pressure vessels were heated to 150 °C for 1–7 days. Reactions were either quenched by allowing the oven to cool to room temperature naturally or cooled slowly to room temperature at rates ranging between 0.3 °C/h and 1 °C/h. Products were left in the pouches at room temperature for an additional 1–4 weeks to promote crystallization. Pouches were opened in air, and the products were recovered via vacuum filtration.

The NCS polymorph was synthesized with 0.3740 g (3.699×10^{-3} mol) of KNO_3, 0.2000 g (8.004×10^{-4} mol) of Na_2NbOF_5, and 0.48 mL, 0.96 mL, or 1.5 mL H_2O. Crystals were clear and colorless. A small amount of white powder was also identified as the CS $KNaNbOF_5$ polymorph.

The CS polymorph was synthesized with 0.0643 g (6.360×10^{-4} mol) of KNO_3, 0.2001 g (8.008×10^{-4} mol) of Na_2NbOF_5, and 0.48 mL of H_2O. A small amount of white powder was also present but could not be identified.

Na_2NbOF_5 was synthesized through the reaction of 0.1344 g NaF, 0.4252 g Nb_2O_5, and 1.2 mL HF. Yields of Na_2NbOF_5 are increased by allowing the product to crystallize for seven days before filtration [22].

2.2. Powder X-ray diffraction

Products were identified using a Rigaku Ultima IV powder diffractometer. Samples were mounted on glass slides.

2.3. Piezoelectric measurements

The conventional Berlincourt method was implemented to make the d_{33} measurements. This method works by applying a mechanical vibration to the sample and recording the resulting charge accumulation on each face [23]. A standard lead zirconate titanate (PZT) sample was used to calibrate the PM3500 d_{33} meter from KCF Technologies. The room temperature d_{33} measurement was performed at a frequency of 100 Hz with a force of 24.8 mN. The relative dielectric permittivity values were calculated using the well-known capacitance formula $C = \frac{\varepsilon_0 \varepsilon_r A}{d}$ with data collected from an Agilent E4980A Precision LCR meter.

Broadband electrical impedance measurements were performed to determine the extent of piezoelectric resonance in single crystals of $KNaNbFO_5$. The single crystals were coated with silver paint on opposing parallel flat faces and air-dried to form a parallel plate capacitor (metal insulator metal, MIM) with good electrical contacts and a typical capacitance of 167 fF. The piezoelectric resonance characteristics of the MIM were analyzed at room temperature using an Agilent 4294A precession impedance analyzer (PIA). The magnitude and the phase angle of the impedance were both collected from 100 kHz to 5 MHz. The resonance and antiresonance frequencies were obtained by fitting the peaks observed in the admittance and impedance plots to a Gaussian function. Owing to the irregular dimensions of the typical crystals, the effective electromechanical coupling coefficient k_{eff}^2 was calculated using Eq. (1)

$$k_{eff}^2 \approx \frac{f_n^2 - f_m^2}{f_n^2} \qquad (1)$$

where f_n^2 is the resonance frequency and f_m^2 is the antiresonance frequency [24]. This equation assumes a mechanical quality factor greater than 100 [24]. This is a reasonable assumption given the number of overtones and the suitable FWHM (~675 kHz, < 0.5%) of the main resonant peak.

2.4. Triboluminescence

Crystals of $KNaNbOF_5$ were crushed between two glass slides. A multimode fiber optic bundle transported the light to an Andor i303 Czerny–Turner monochromator. The sample was manually crushed between the slides while the spectrum was recorded with an Andor DU420A-BEX2-DD CCD. See Supporting information for a video clip capturing the triboluminescence.

3. Results and discussion

3.1. Crystal growth

The first consideration for crystal growth of the NCS phase of $KNaNbOF_5$ is to ensure that only the desired polymorph crystallizes from solution. We previously showed how a high K:Na ratio, at least greater than 1:1 is needed in the reaction solution to synthesize the NCS polymorph [11]. Crystal growth solutions therefore contained a K:Na ratio of about 2.3:1 to ensure the NCS polymorph would crystallize. Three other desirable conditions in solution crystal growth include high yield, few (ideally one) nucleation sites, and crystal clarity. The heating time, cooling rate, and concentration were varied to determine optimal crystal growth conditions to yield a large single crystal. The concept of creating a pinhole at the top of sealed pouches is also introduced to examine if the pinhole would affect crystal growth via transfer of water from the water backfill to contents within the pouch. General trends are summarized in Table 1.

Reactions that contained 0.96 mL of water resulted in a greater number of crystals, which suggests that a lower concentration of reactants results in a greater number of nucleation sites. Reactions that contained 1.5 mL of water yielded products that could not be identified. The Teflon film is semi-permeable to water above 100 °C and water from the backfill can enter the pouch during the reaction. The mass of the pouches was measured before and after the reactions. Pinholes are expected to increase the amount of water that enters the pouch and therefore can influence crystal

Please cite this article as: K.B. Chang, et al., J. Solid State Chem. (2015), http://dx.doi.org/10.1016/j.jssc.2015.07.011

Table 1
Effect of synthetic conditions on NCS $KNaNbOF_5$ crystal growth.

Synthetic condition	Effect on crystal growth
Higher reactant concentration	Fewer number of crystals
Increase dwell time at elevated temperature	Increase overall yield
Pinholes in pouches	Lower quality crystals
Increase cooling rate	Larger crystals
Increase room temperature crystallization time	Larger crystals

growth. Additionally, if the pinholes are made at the top of the pouch, water will enter though the top and could create a concentration gradient. The mass increase in pouches without pinholes ranged between 0.0084 g and 1.3174 g with an average water uptake of 0.43 g, and no obvious trends between water uptake and reaction time were found. In contrast, the change in mass of pouches with pinholes was found to be dependent on the reaction time. Reactions held at 150 °C for one day showed mass increases ranging from 0.9480 g to 1.8598 g with an average increase of 1.30 g. The pouches with pinholes held at 150 °C for one week had negligible changes in mass. It is possible that over the course of one week, some of the dissolved solids escape the pouch through the pinhole. This loss in mass may compensate for the water entering the pouch, resulting in almost no net mass change. Reactions with pinholes in pouches generally yielded lower quality (more opaque) crystals than those reactions without pinholes.

Reactions held at 150 °C for 1 week gave a higher yield of $KNaNbOF_5$ crystals than those held for 1 day. The largest crystal was grown from a reaction held at 150 °C for 1 week. After the dwell period, the oven was turned off and the autoclave was allowed to cool at the natural rate of the oven. This reaction yielded three large crystals with masses of 0.0283 g, 0.0137 g, and 0.0067 g. The crystals are shown in Fig. 1. It is interesting to note that contrary to typical crystallization behavior, a more concentrated reaction mixture and a faster cooling rate resulted in fewer and larger crystals. Additional experiments that examine temperature and concentration gradients are required to determine the role of diffusion and nucleation on nucleation sights and crystal growth. Higher yields with longer dwell times may be indicative of the slow formation of a complex building unit needed for the crystallization of the final product. Future *in situ* solution studies to characterize the evolution of the dissolved species would give great insight toward the crystallization of these materials.

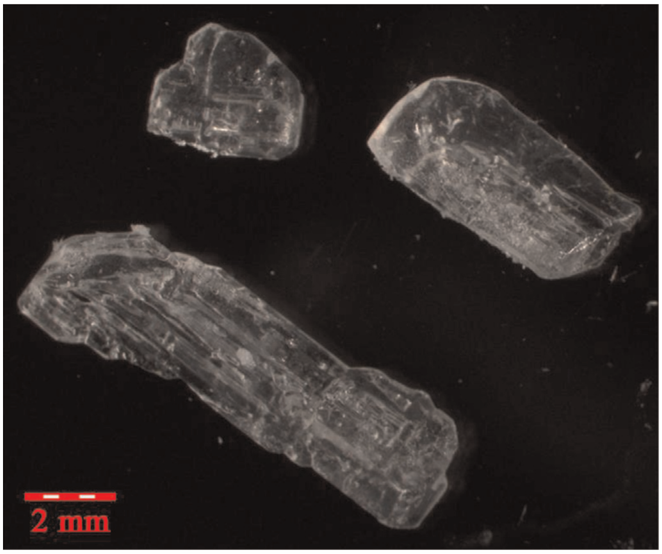

Fig. 1. Single crystals of NCS $KNaNbOF_5$. The largest crystal shown was used for piezoelectric measurements.

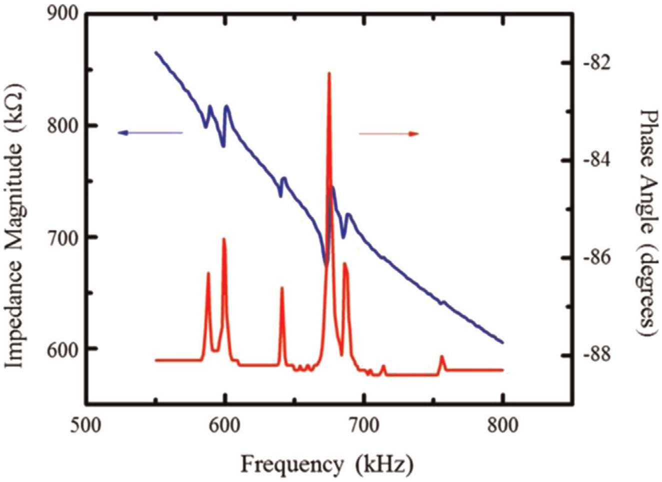

Fig. 2. Room temperature impedance spectrum from 550 to 800 kHz for a single crystal of NCS $KNaNbOF_5$.

3.2. Piezoelectricity

Room temperature impedance spectra performed on single crystals from 550 to 800 kHz and 1 to 3 MHz are given in Figs. 2 and 3a, respectively. The fundamental and related satellite peaks at the lower frequencies in Fig. 2 correspond to planar mode resonances. The higher frequency resonance modes shown in Fig. 3a correspond to thickness resonance modes. The parameters f_m and f_n in Eq. (1) correspond to the frequency at which the equivalent circuit operates at minimum and maximum impedance, respectively [24]. A more detailed view of the main resonance peak around 2 MHz is shown in Fig. 3b. Minor resonance modes become apparent and are likely the result of geometric imperfections or inclusions in the crystals tested.

These geometrical imperfections are observable under polarized light microscopy as seen in Fig. 4. These optical path disturbances may be the result of internal stresses present during the crystal growth process and create a sample with a difference in effective indices of refraction in the x and y directions, birefringence, seen as varying colors that highlight these sites. Continued refinement to the crystal growth process could lead to the minimization of such defects and yield an impedance spectrum that is less cluttered by these minor resonance modes [25,26].

$KNaNbOF_5$ crystals yielded a d_{33} value of ± 6.3 pCN^{-1}. When compared to other commonly used piezoelectrics, such as barium titanate (BTO) and PZT as seen in Table 2, it is clear that the piezoelectric coefficient of $KNaNbOF_5$ is much lower. However, its value is higher and more comparable to other systems such as the d_{11} of α-quartz. The room temperature relative permittivity of $KNaNbOF_5$ measured at 1 kHz was found to be around 7.2 with a loss tangent of 0.01. The low permittivity value is not unexpected given the relatively small and stiff dipoles within the $[NbOF_5]^{2-}$ anion. Moreover, while the measured loss is relatively low, it is anticipated that the intrinsic loss of the material is much lower. Given the small crystal size, samples of the ideal area to thickness ratios for dielectric measurements were not attainable, and the shape irregularity of the crystals can contribute extrinsically to the observed dielectric loss.

Table 3 summarizes the k_{eff} calculations from the data seen in Figs. 2 and 3 and includes a comparison with commonly used piezoelectric materials. While a high k_{eff} is needed for commercial applications that incorporate mechanical power, use of $KNaNbOF_5$ in applications such as signal filters may be more appropriate owing to the poor mechanical properties of these crystals.

Please cite this article as: K.B. Chang, et al., J. Solid State Chem. (2015), http://dx.doi.org/10.1016/j.jssc.2015.07.011

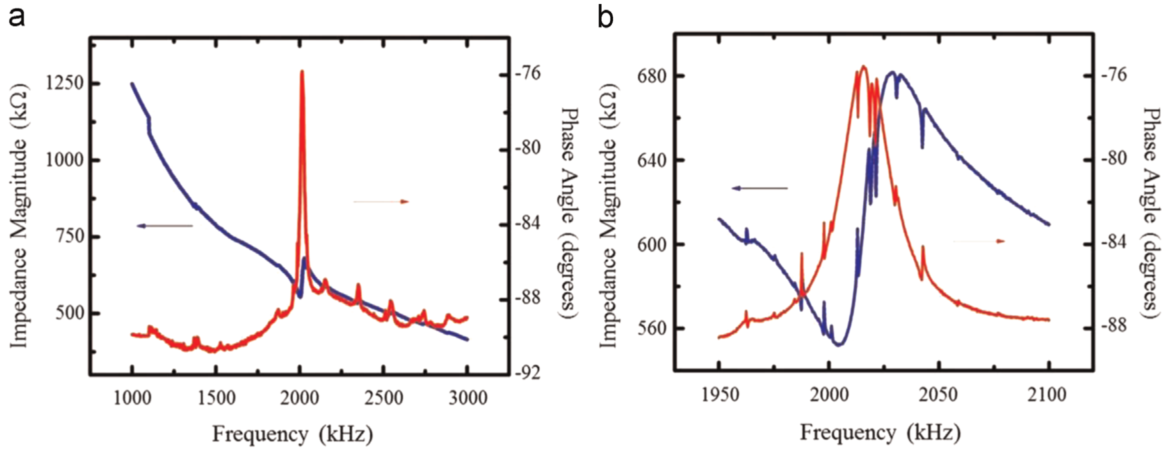

Fig. 3. (a) Room temperature impedance spectrum from 1 to 3 MHz for a single crystal of NCS $KNaNbOF_5$. (b) A more detailed view of the main resonance peak at about 2 MHz.

Compared to a previously studied oxide-fluoride system, [29] these crystals show a higher k_{eff} value, making them a more attractive option in sensor applications.

3.3. Triboluminescence

Mechanisms for TL can fall broadly into two categories. The first involves a discharge through air or another atmosphere. The second is from other processes within the bulk of the crystal, such as defect recombination or piezoelectric polarization. The first mechanism involving a gas discharge can be identified through 1) N_2 emission lines in the TL spectrum, 2) suppression of TL under a N_2 free atmosphere, or 3) suppression of TL when fractured while submerged in a liquid. If none of these conditions are met, TL within a material is likely rooted from some processes within the bulk of the crystal [31].

The TL spectrum of $KNaNbOF_5$ is shown in Fig. 5, which shows one broad peak centered around 510 nm. No spectral features are observed between 300 and 400 nm, which would have been indicative of nitrogen emission. To confirm that a nitrogen atmosphere is not required to observe TL in this material, crystals were crushed in an Ar atmosphere and while submerged under hexanes, isopropanol, and water. Triboluminescence persisted in these experiments, indicating that TL likely not a result of photoluminescence caused by UV excitation from N_2 emission. Samples were excited with a 325 and 442 nm dual wavelength helium–cadmium laser and no photoluminescence was observed, supporting that the TL of this material is not related to a photoluminescence mechanism.

To determine if the TL originates from the piezoelectric effect, crystals of the CS polymorph were also crushed. A TL effect was observed and similar to the NCS polymorph, TL persisted when crushed in an Ar atmosphere and while submerged under hexanes, isopropanol, and water. The TL observed signal of the CS polymorph, however, could not be recorded. The CS polymorph was also found to not exhibit any photoluminescence. Because TL is observed in the CS polymorph, the piezoelectric effect is likely not the origin of the TL. Instead, TL may originate from crystal defects or be related to an electroluminescence effect.

Table 2
Relative permittivity and d_{33} values of NCS $KNaNbOF_5$ compared with other piezoelectrics.

Sample	d_{33} ($\pm$ pCN^{-1})	Relative permittivity
$KNaNbOF_5$	6.3	7.1
Standard PZT	453	850
PVDF	22 [27]	10.85 [28]
$Na_{0.5}K_{0.5}NbO_3$ [24]	160	400
α-quartz [24]	2.3[a]	4.6
BTO [24]	190	1900
PZT A [24]	268	1200
PZT B [24]	480	2800

[a] signifies a d_{11} value.

4. Conclusions

Large single crystals of both polymorphs of $KNaNbOF_5$ were grown under hydrothermal conditions using our previously developed synthetic principles. Single crystals allowed

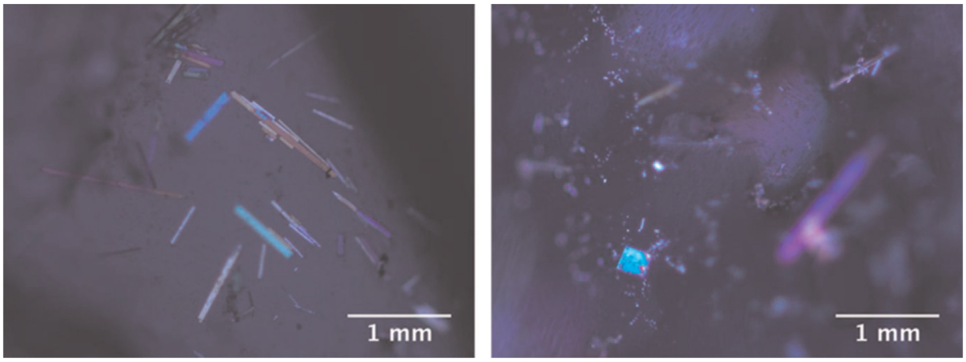

Fig. 4. Optical microscope images of crystal imperfections within NCS $KNaNbOF_5$ single crystals take under polarized light. Images were taken at 100 × linear magnification under diascopic dark field conditions.

Please cite this article as: K.B. Chang, et al., J. Solid State Chem. (2015), http://dx.doi.org/10.1016/j.jssc.2015.07.011

Table 3
k_{eff} values of NCS $KNaNbOF_5$ compared to other piezoelectrics.

Sample	Frequency range (kHz)	$f_{m(\mathrm{kHz})}$	$f_{n(\mathrm{kHz})}$	$k_{eff}{}^2(\times10^{-3})$	k_{eff}
This system	665–683	672.5	678.0	16.16	0.1271
This system	1960–2080	2005	2030	24.47	0.1565
$[Hdpa]_2NbOF_5\cdot2H_2O$ [29],[a]	407–415	411.5	413.0	6.978	0.084
$[Hdpa]_2NbOF_5\cdot2H_2O$ [29],[a]	975–990	983.3	985.3	4.095	0.064
SiOF [30]	–	–	–	101	0.318
$Na_{0.5}K_{0.5}NbO_3$ [24]	–	–	–	–	0.53[b]
α-quartz [24]	–	–	–	–	0.1[c]
BTO [24]	–	–	–	–	0.49[b]
PZT A [24]	–	–	–	–	0.68[b]
PZT B [24]	–	–	–	–	0.72[b]

[a] dpa=2,2′-dipyridylamine.
[b] k_{33} values.
[c] k_{11} values.

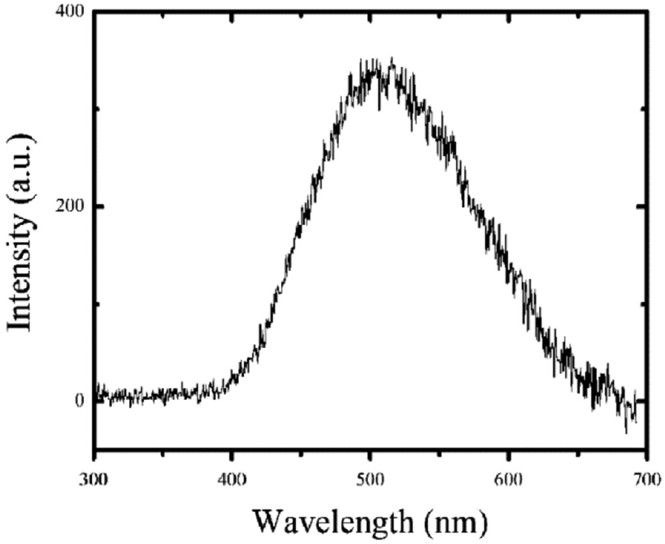

Fig. 5. Triboluminescence spectrum of NCS $KNaNbOF_5$.

measurements of piezoelectricity and TL. The d_{33} value of the NCS $KNaNbOF_5$ was measured to be ±6.3 pCN^{-1}. The TL was also found to persist when crystals were crushed while submerged in a liquid or under an Ar atmosphere. The NCS $KNaNbOF_5$ polymorph also did not photoluminesce under UV excitation and the TL spectrum did not show peaks associated with N_2 gas emission. Furthermore, the CS polymorph also produced TL through a mechanism unassociated with N_2 gas emission. The TL of the NCS $KNaNbOF_5$ polymorph is therefore likely not a result of piezoelectric polarization within the crystal.

Acknowledgments

The authors gratefully acknowledge support from the National Science Foundation (DMR-1307698). This work made use of the J. B. Cohen X-ray Diffraction Facility and the Magent, Low Temperature, and Optical Facility supported by the MRSEC program of the National Science Foundation (DMR-1121262) at the Materials Research Center of Northwestern University. JCN and BE would like to acknowledge support by the National Science Foundation (DMR-120793). L.F. acknowledges NSF IGERT DGE-0801685 and the Institute for Sustainability and Energy at Northwestern (ISEN). E.J.L. was supported by the National Science Foundation MRSEC (DMR-1121262) and T.K.S. was in part supported by the U.S. Department of Energy, BES (DE-SC0012130). N.P.S. acknowledges support as an Alfred P. Sloan Research Fellow.

Appendix A. Supplementary material

Supplementary data associated with this article can be found in the online version at http://dx.doi.org/10.1016/j.jssc.2015.07.011.

References

[1] J.T. Dickinson, L. Scudiero, K. Yasuda, M.-W. Kim, S.C. Langford, Tribol. Lett. 3 (1997) 53.
[2] K. Nakayama, H. Hashimoto, Wear 185 (1995) 183.
[3] C.N. Xu, T. Watanabe, M. Akiyama, Appl. Phys. Lett. 74 (1999) 1236.
[4] J.I. Zink, Acc. Chem. Res. 11 (1978) 289.
[5] J.T. Dickinson, L.B. Brix, L.C. Jensen, J. Phys. Chem. 88 (1984) 1698.
[6] L.M. Sweeting, Chem. Matters 8 (1990) 10.
[7] F. Bortolani, A. del Campo, J.F. Fernandez, F. Clemens, F. Rubio-Marcos, Chem. Mater. 26 (2014) 3838.
[8] L. Egerton, D.M. Dillon, J. Am. Ceram. Soc. 42 (1959) 438.
[9] F. Rubio-Marcos, P. Ochoa, J.F. Fernandez, J. Eur. Ceram. Soc. 27 (2007) 4125.
[10] X. Wang, J. Wu, D. Xiao, J. Zhu, X. Cheng, T. Zheng, B. Zhang, X. Lou, X. Wang, J. Am. Chem. Soc. 136 (2014) 2905.
[11] K.B. Chang, A. Vinokur, R.A. Pinlac, M.R. Suchomel, M.R. Marvel, K. R. Poeppelmeier, Inorg. Chem. 53 (2014) 6979.
[12] Crystal Growth: An Introduction, in: P. Hartman (Ed.), North-Holland Publishing Company, Amsterdam, 1973.
[13] C.D. McMillen, J.W. Kolis, Philos. Mag. 92 (2012) 2686.
[14] T.F. Antokhina, L.N. Ignat'eva, N.N. Savchenko, I.A. Tkachenko, T.A. Kaidalova, Zhurnal Neorg. Khimii 48 (2003) 551.
[15] M.R. Marvel, J. Lesage, J. Baek, P.S. Halasyamani, C.L. Stern, K.R. Poeppelmeier, J. Am. Chem. Soc. 129 (2007) 13963.
[16] R.A.F. Pinlac, C.L. Stern, K.R. Poeppelmeier, Crystals 1 (2011) 3.
[17] A.D. Vasiliev, N.M. Laptash, J. Struct. Chem. 53 (2012) 902.
[18] J.C. Bertolini, J. Emerg. Med. 10 (1992) 163.
[19] D. Peters, R. Miethchen, J. Fluor. Chem. 79 (1996) 161.
[20] E.B. Segal, Chem. Health Saf. 7 (2000) 18.
[21] W.T.A. Harrison, T.M. Nenoff, T.E. Gier, G.D. Stucky, Inorg. Chem. 32 (1993) 2437.
[22] R. Stomberg, Acta Chem. Scand. Ser. A 38 (1984) 603.
[23] P. Groen, J. Holterman, An Introduction to Piezoelectric Materials and Applications, Stichting Applied Piezo, Apeldoorn, The Netherlands, 2013.
[24] A.J. Moulson, J.M. Herbert, Electroceramics, Chapman and Hall, New York, NY, 1990.
[25] L. Labonté, D. Pagnoux, P. Roy, F. Bahloul, M. Zghal, Opt. Commun. 262 (2006) 180.
[26] M. Zghal, Opt. Eng. 46 (2007) 128002.
[27] L. Huang, C. Lu, F. Wang, L. Wang, RSC Adv. 4 (2014) 45220.
[28] L. Wu, J. Alamuse, J. Xue, T. Itoni, N. Hu, Y. Li, C. Yan, J. Qui, H. Ning, W. Yuan, B. Gu, J. Intell. Mater. Syst. Struct. *25* (2013) 1813.
[29] H. Lu, R. Gautier, M.D. Donakowski, T.T. Tran, B.W. Edwards, J.C. Nino, P. S. Halasyamani, Z. Liu, K.R. Poeppelmeier, J. Am. Chem. Soc. 135 (2013) 11942.
[30] S. Matsuda, M. Hara, M. Miura, T. Matsude, U.M. Ueda, Y. Satoh, K. Hashimoto, IEEE Trans. Ultrason. Ferroelectr. Freq. Control 59 (2012) 135.
[31] L.M. Sweeting, Chem. Mater. 13 (2001) 854.

Please cite this article as: K.B. Chang, et al., J. Solid State Chem. (2015), http://dx.doi.org/10.1016/j.jssc.2015.07.011